Differential role of GABAA receptors and neuroligin 2 for perisomatic GABAergic synapse formation in the hippocampus

Panzanelli, Patrizia ; Früh, Simon ; Fritschy, Jean-Marc

Abstract: Perisomatic GABAergic synapses onto hippocampal pyramidal cells arise from two populations of basket cells with different neurochemical and functional properties. The presence of the dystrophin-glycoprotein complex in their postsynaptic density (PSD) distinguishes perisomatic synapses from GABAergic synapses on dendrites and the axon-initial segment. Targeted deletion of neuroligin 2 (NL2), a transmembrane protein interacting with presynaptic neurexin, has been reported to disrupt postsynaptic clustering of GABAA receptors (GABAAR) and their anchoring protein, gephyrin, at perisomatic synapses. In contrast, targeted deletion of Gabra2 disrupts perisomatic clustering of gephyrin, but not of 1-GABAAR, NL2, or dystrophin/dystroglycan. Unexpectedly, conditional deletion of Dag1, encoding dystroglycan, selectively prevents the formation of perisomatic GABAergic synapses from basket cells expressing cholecystokinin. Collectively, these observations suggest that multiple mechanisms regulate formation and molecular composition of the GABAergic PSD at perisomatic synapses. Here, we further explored this issue by investigating the effect of targeted deletion of Gabra1 and NL2 on the dystrophin-glycoprotein complex and on perisomatic synapse formation, using immunofluorescence analysis with a battery of GABAergic pre- and postsynaptic markers. We show that the absence of 1-GABAAR increases GABAergic synapses containing the 2 subunit, without affecting the clustering of dystrophin and NL2; in contrast, the absence of NL2 produces highly variable effects postsynaptically, not restricted to perisomatic synapses and being more severe for the GABAAR subunits and gephyrin than dystrophin. Altogether, the results confirm the importance of NL2 as organizer of the GABAergic PSD and unravel distinct roles for 1- and 2-GABAARs in the formation of GABAergic circuits in close interaction with the dystrophin-glycoprotein complex.

DOI: https://doi.org/10.1007/s00429-017-1462-7

Originally published at:
Panzanelli, Patrizia; Früh, Simon; Fritschy, Jean-Marc (2017). Differential role of GABAA receptors and neuroligin 2 for perisomatic GABAergic synapse formation in the hippocampus. Brain Structure Function, 222(9):4149-4161.
DOI: https://doi.org/10.1007/s00429-017-1462-7

Differential role of $GABA_A$ receptors and neuroligin 2 for perisomatic GABAergic synapse formation in the hippocampus

Patrizia Panzanelli[1], Simon Früh[2,3] and Jean-Marc Fritschy[2,3*]

[1]Department of Neuroscience Rita Levi Montalcini, University of Turin, 10124 Turin, Italy

[2]Institute of Pharmacology and Toxicology, University of Zurich, 8057 Zurich, Switzerland

[3]Neuroscience Center Zurich, University of Zurich and Federal Institute of Technology, 8057 Zurich, Switzerland

*Corresponding author: Jean-Marc Fritschy, Institute of Pharmacology and Toxicology, Winterthurerstrasse 190, 8057 Zurich, Switzerland; fritschy@pharma.uzh.ch

Conflict of interest: The authors declare no competing financial interests.

Orcid ID

PP: 0000-0002-5127-2757

SF: 0000-0001-6804-5385

JMF: 0000-0002-8552-3702

Acknowledgements: This work was supported by the Swiss National Science Foundation (Grant 310030_146120 to JMF). We thank Dr. Shiva K. Tyagarajan for scientific discussion and Dr. Tatjana Haenggi and Cornelia Schwerdel for technical support and mouse genotyping.

Conflicts of interest: the authors declare to have no conflict of interest.

Abstract

Two populations of basket cells form perisomatic GABAergic synapses onto hippocampal pyramidal cells, with different neurochemical and functional properties, to regulate hippocampal network oscillatory activity. These synapses are molecularly distinct from GABAergic synapses on dendrites and the axon-initial segment, notably by the presence of the dystrophin-glycoprotein complex in the postsynaptic density (PSD). Targeted deletion of neuroligin 2 (NL2), a transmembrane protein interacting with presynaptic neurexin, disrupts postsynaptic clustering of $GABA_A$ receptors ($GABA_AR$) and their anchoring protein, gephyrin, at perisomatic synapses. In contrast, targeted deletion of *Gabra2* disrupts perisomatic clustering of gephyrin, but not of α1-$GABA_AR$, NL2, or dystrophin/dystroglycan. Unexpectedly, conditional deletion of *Dag1*, encoding dystroglycan, selectively prevents formation of GABAergic synapses from basket cells expressing cholecystokinin. Collectively, these findings suggest that multiple mechanisms regulate formation and molecular composition of the GABAergic PSD at perisomatic synapses. Here, we investigated the effect of targeted deletion of *Gabra1* and NL2 on the dystrophin-glycoprotein complex and on perisomatic synapse formation, using immunofluorescence analysis with a battery of GABAergic pre- and postsynaptic markers. We show that absence of α1-$GABA_AR$ increases GABAergic synapses containing the α2 subunit, without affecting the clustering of dystrophin and NL2; in contrast, absence of NL2 produces highly variable effects postsynaptically, not restricted to perisomatic synapses and being most severe for the α2 subunit and gephyrin. Altogether, the results confirm the importance of NL2 as organizer of the GABAergic PSD and unravel distinct roles for α1- and α2-$GABA_ARs$ in the formation of GABAergic circuits in close interaction with the dystrophin-glycoprotein complex.

Key words: dystrophin glycoprotein complex; gephyrin; vesicular GABA transporter; cholecystokinin; parvalbumin

Introduction

Pyramidal cells, the principal neurons of the cerebral cortex and hippocampus, receive segregated GABAergic inputs on dendrites, the soma and the axon initial segment (AIS), arising from distinct populations of interneurons and exerting differential effects on their function and firing properties. Although it is well established that proteins of GABAergic postsynaptic densities (PSD), especially $GABA_A$ receptors ($GABA_AR$), are molecularly heterogeneous across cell types and synapses in different cellular compartments, the mechanisms underlying the formation and regulation of distinct GABAergic PSD are poorly understood. In pyramidal cells, the dystrophin-glycoprotein complex (DGC) is largely restricted to perisomatic synapses formed by basket cell terminals (Knuesel et al. 1999). It is not present in synapses of the AIS or on distal dendrites (Panzanelli et al. 2011). The DGC is composed of α- and β-dystroglycan, dystrophin, and variants of dystrobrevin and syntrophins. It is involved in cell adhesion, extracellular signaling and intracellular signaling to regulate the clustering of regulatory proteins and anchoring to the actin cytoskeleton (Waite et al. 2009). In neurons, α-dystroglycan interacts with neurexin isoforms (presynaptically), while dystrophin might interact indirectly with neuroligin 2 (NL2), a postsynaptic adhesion protein at GABAergic synapses, via SynArfGEF and S-SCAM (reviewed in (Tyagarajan and Fritschy 2014)). The contrast between the widespread distribution of NL2 across most GABAergic synapses and the DGC selectively in perisomatic synapses raised the possibility for a specific function of this interaction in basket cell synapses. In support for this possibility, the morphological analysis of neuroligin2-knockout (NL2-KO) mice revealed a selective loss of $GABA_AR$ and gephyrin in the pyramidal cell layer of CA1 (Poulopoulos et al. 2009). However, it was not tested whether the localization of the DGC was affected.

Further support for a specific role of the DGC at perisomatic synapses arose from our own study in mice with a targeted deletion of *Gabra2* (α2-KO), which demonstrated a striking difference in the postsynaptic clustering of the $GABA_AR$ α1 subunit and NL2 in perisomatic and dendritic synapses of CA1 pyramidal cells (Panzanelli et al. 2011). In brief, we showed

that α1-$GABA_AR$ and NL2 remain clustered postsynaptically, along with dystrophin and dystroglycan in perisomatic synapses of α2-KO mice, while being largely absent from dendritic synapses. As this subcellular difference correlated precisely with the presence of the DGC, we inferred the existence of synapse-specific anchoring of $GABA_ARs$ at postsynaptic sites and suggested that the DGC might contribute to stabilize α1-$GABA_AR$ and NL2, but not gephyrin, in perisomatic PSD (Fritschy et al. 2012). Further, these results suggested a preferential interaction between α2-$GABA_AR$ and gephyrin compared to α1-$GABA_AR$, in line with the difference in binding affinity of these two subunits to gephyrin.

Nevertheless, it remains unclear why $GABA_AR$ and gephyrin clustering is more severely affected in perisomatic than dendritic GABAergic synapses in NL2-KO mice. Furthermore, the formation of distinct molecular complexes within single GABAergic synapses, segregated according to the $GABA_AR$ subtype when the DGC is present, remains purely speculative.

A further complication arises from our recent observation that dystroglycan is required not so much for stabilizing $GABA_ARs$ and NL2 postsynaptically, but rather, and selectively, for the formation of GABAergic synapses from CCK-positive basket cells, recognized by their high content of cannabinoid type 1 receptors (CB1) and the type 3 vesicular glutamate transporter (VGLUT3)(Früh et al. 2016). Therefore, it is necessary to investigate molecular heterogeneity of synapses in a broader context, involving also presynaptic afferents. The relevance of these issues is underscored by the fact that genetic alterations of the DGC (affecting either dystrophin or dystroglycan) are accompanied by intellectual disabilities (Waite et al. 2012) and that mutations of NL2 are found in some forms of autism-spectrum disorder (Baudouin 2014). In addition, perisomatic GABAergic synapses formed by the two subpopulations of basket cells (CCK-basket cells versus parvalbumin basket cells) have fundamentally different roles in the regulation of network activity in the hippocampus (Klausberger et al. 2005).

In the present study, we aimed at further characterizing the molecular heterogeneity of perisomatic and dendritic synapses in CA1 pyramidal cells and testing the hypothesis of a preferential interaction of the DGC with α1-$GABA_AR$ and NL2. Using mice lacking either the

$GABA_AR$ α1 subunit (α1-KO) or NL2 (NL2-KO), we investigated how the constitutive absence of these proteins impacts on perisomatic synapse formation and postsynaptic clustering of $GABA_AR$, gephyrin, NL2, and the DGC.

Materials and Methods

Animals

Experiments were conducted in accordance with Swiss law on animal experimentation and the European Parliament Directive of 22 September 2010 on the protection of animals used for scientific purposes (2010/63/EU) and were approved by the cantonal veterinary office of Zurich. For morphological analysis, α1-KO and NL2-KO mice maintained on a heterozygote background and bred at the Laboratory Animal Services Center (LASC) of the University of Zurich were used. The mice were obtained from Dr. Greg Homanics (α1-KO) and Dr. Nils Brose (NL2-KO) and have been extensively characterized previously (Kralic et al. 2006; Schneider Gasser et al. 2007; Poulopoulos et al. 2009). All genotyping was performed by PCR analysis of tail/ear biopsies.

Tissue preparation

For regional distribution and high resolution analysis of synaptic proteins, adult mice of both sexes (2-3 months-old) were deeply anesthetized with pentobarbital (Nembutal, 50 mg/kg, i.p.) and perfused transcardially with ice-cold artificial cerebrospinal fluid, as described (Notter et al. 2014). The mice were then decapited and the brain taken out on ice. A block containing the entire hippocampal formation was fixed by immersion in 4% paraformaldehyde in 0.15 M Na-phosphate buffer, pH 7.4 at 4°C for 90 min. After fixation, the tissue was cryoprotected in 30% buffered sucrose, frozen, and sectioned at 40 μm with a sliding microtome. Free-floating sections were stored in anti-freeze solution at -20ºC until use.

Immunofluorescence staining and confocal laser scanning microscopy

High sensitivity detection of synaptic proteins was achieved in these mildly-fixed tissue sections processed for triple immunofluorescence staining, as described (Panzanelli et al. 2009; Schneider Gasser et al. 2006), using various combinations of primary antibodies raised in different species (Table 1). All secondary antibodies were raised in goat and conjugated to Alexa488 (Molecular Probes), Cy3 (Jackson Immunoresearch, West Grove, PA), or Dylight 647 (Molecular Probes).

Images from the CA1 pyramidal layer and stratum radiatum were acquired by confocal laser scanning microscopy (LSM 700 and LSM 710 Zen, Carl Zeiss AG) using sequential acquisition of separate wavelength channels to avoid fluorescence crosstalk. Stacks of 10-12 confocal sections (1024 x 1024 pixels; 70-120 nm/pixel) spaced 500-800 nm were acquired with a Panfluor oil-immersion 40x objective (numerical aperture 1.4) with the pinhole set at 1 Airy unit. For display, images were processed with ImageJ or Imaris software (Bitplane, Switzerland).

Antibody characterization

Primary polyclonal antibodies against synthetic peptide sequences derived from the $GABA_AR$ α1, α2 and γ2 subunits cDNAs were raised in house (Fritschy and Mohler 1995). The following peptides sequences were used: α1 subunit residues 1-16, α2 subunit residues 1-9 and γ2 subunit residues 1-16. All antibodies were raised in guinea pigs. They were characterized extensively by biochemistry (Western blotting, immunoprecipitation) and by immunohistochemistry using tissue from α1-, α2- and γ2-KO mice (Benke et al. 1996; Benke et al. 1991; Fritschy and Mohler 1995; Kralic et al. 2006; Lagier et al. 2007; Panzanelli et al. 2011; Gunther et al. 1995).

The mouse monoclonal mAb7a against gephyrin was raised using affinity-purified rat glycine receptors. It is widely used to detect gephyrin in inhibitory synapses, as well as recombinant gephyrin expressed in neurons (Lardi-Studler et al. 2007; Sassoè-Pognetto and Fritschy 2000).

The affinity-purified rabbit polyclonal antibody against VGAT was raised using a rat synthetic peptide 75-87 (AEPPVEGDIHYQR). Its specificity for the mammalian VGAT was demonstrated by Western blotting and immunohistochemistry (selective detection of GABAergic terminals in CNS sections and primary neuron cultures) (Brünig et al. 2002; Dumoulin et al. 1999).

The guinea pig polyclonal serum against VGLUT3 was raised using a synthetic peptide from rat VGLUT3 protein. Its specificity was determined by comparison with the staining pattern

obtained with other VGLUT3 antisera (Fremeau et al. 2002); preadsorption with the immunogen peptide eliminates all immunostaining.

The rabbit polyclonal antiserum against cannabinoid receptor 1 (CB1-R) was raised using a synthetic peptide from rat cannabinoid receptor 1 (residues 401-473). Its specificity was demonstrated by Western blotting and immunohistochemistry (Morini et al. 2015).

The monoclonal C-terminal anti-dystrophin antibody (NCL-Dys1) recognizes all dystrophin isoforms (Knuesel et al. 2000). It reacts strongly with the rod domain (between residues 1181-1388) of human dystrophin.

The rabbit polyclonal antibody against NL2 (gift from P. Scheiffele) was raised using a synthetic peptide antigen: N-(C)-RGGGVGADPAEALRPACP-C, corresponding to amino acids 750–767 in the cytoplasmic domain of mouse NL2 (splice variant A) (Budreck and Scheiffele 2007). Its specificity is confirmed by the complete loss of immunostaining in tissue from NL2-KO mice.

The mouse monoclonal antibody against parvalbumin was raised from purified bovine parvalbumin. Its specificity was demonstrated by western blotting and immunohistochemistry, (Celio 1990), as well as in parvalbumin-KO mice.

Image analysis

Quantification of the number of clusters positive for the $GABA_AR$ $\alpha1$, $\alpha2$ and $\gamma2$ subunits, gephyrin, NL2, dystrophin, CB1, VGLUT3 and VGAT in the CA1 area was performed in single 8-bit confocal images using the software Image J (NIH), using high-resolution images obtained from 3-6 mice per genotype and staining combination. Clusters were identified with a custom-made macro, based on intensity relative to background and size (minimal area, 0.1 μm^2). The outlines of clusters were inserted in a mask used for measuring the mean intensity of each cluster in addition to its area. The analysis of single and double labeled clusters was performed separately in the pyramidal cell layer and stratum radiatum. Owing to the variability of the results, some combinations were repeated up to 6 times, using 2-4 mice per genotype in each experiment. In the pyramidal cell layer, cluster density per surface area

was assessed in single confocal images, whereas on the AIS, cluster density per unit length was assessed in 3D reconstructions from stacks of 6-12 images spanning a thickness of 3-4 μm. Data are reported as mean ± SEM (N=number of mice). Statistical analyses were done with the software Prism (Version 4; GraphPad, San Diego, CA). Differences in numerical density of clusters across genotypes were performed using unpaired t-test and Mann-Whitney test; changes in cluster size were tested using cumulative distribution analysis and the Kolmogorov-Smirnov test; linear correlation analysis was performed to compare the staining intensity of postsynaptic clusters across genotypes.

Results

α1-KO mice

To determine whether the targeted inactivation of *Gabra1*, which is abundantly expressed in both pyramidal cells and a subset of interneurons in the CA1 region of the hippocampus, had an effect on the postsynaptic clustering of other proteins, we examined immunohistochemically the distribution of GABAergic postsynaptic markers in hippocampal formation of adult mice. Our previous results in α2-KO mice had revealed a layer-specific reduction of GABAergic postsynaptic markers in CA1, except in perisomatic synapses containing the DGC (Panzanelli et al. 2011). For this reason, we analyzed separately the CA1 stratum radiatum (RAD), which is largely devoid of the DGC, and the pyramidal cell layer (PCL), strongly enriched in DGC.

Triple immunofluorescence staining for NL2, the α2 subunit and gephyrin revealed that α1-subunit ablation causes an increase in the density of α2 subunit and gephyrin clusters in both RAD and PCL, whereas clusters positive for NL2 appeared unaltered (Fig.1A-B'''). These descriptive results were confirmed by quantitative analysis in five mice per genotype. The density of α2 subunit and gephyrin clusters was increased by about 30% in the PCL and RAD (PCL: α2 t_4=7.983, p=0.0013, geph t_4=6.802, p=0.0024; RAD: α2 t_4=5.042, p=0.0073, geph t_4=18.67, p<0.0001; unpaired t-test; Table 2). The size of the α2 subunit clusters (as determined by cumulative probability distribution analysis) was also increased (Fig.1C-D') in RAD and PCL of α1-KO mice, but not that of gephyrin or NL2 clusters. In immunofluorescence analyses, the apparent size of a small structure, close to the resolution of the objective, is strongly influenced by its intensity, reflecting the density of antibody binding sites (epitopes) present in it. Therefore, we tested whether the correlation between the size and fluorescence intensity (calculated as the mean intensity of all voxels in the cluster on an 8-bit scale) was different in wildtype and α1-KO mice. For each marker, we observed a linear correlation between cluster size and intensity; however, the slope of this correlation was higher in α1-KO mice for the α2 subunit and NL2, while being unaltered for

gephyrin (Fig.1E-F'; Table 2). Again, this change was similar in RAD and PCL, indicating that synaptic remodeling taking place in the absence of the α1-subunit occurs independently of the presence or absence of the DGC.

The most parsimonious explanation of these results in α1-KO mice is that the α2 subunit substitutes for the α1 subunit in synapses that normally contain both α1- and α2-$GABA_AR$, thereby explaining their increased concentration, and that the α2 subunit also becomes present in synapses that normally contain only the α1 subunit (possibly with low levels of gephyrin). Interestingly, the local density of gephyrin molecules appears to be stable across all these synapses, whereas NL2 is increased in the absence of α1-$GABA_AR$.

To confirm this hypothesis and determine whether the increase in α2 subunit and gephyrin clusters was due to an increase of presynaptic terminals, we used a double staining with gephyrin and VGAT (not shown). The results confirmed the increase of gephyrin cluster density and revealed a modest (20%) increase of VGAT terminals, which was significant only in the PCL (VGAT: t_4=3.624, p=0.0223; unpaired t-test; Table 2) and suggested a net increase in synapse density compared to wildtype mice.

Since the effects of α1 subunit inactivation were very similar in the PCL and RAD, we determined whether the presence of dystrophin was changed in α1-KO mice, along with CB1 and VGLUT3, presynaptic markers of CCK-basket cells (Omiya et al. 2015). Triple immunofluorescence staining was performed for dystrophin, CB1 and VGLUT3 (Fig. 2). Quantitative analysis in five mice per genotype revealed that *Gabra1* inactivation had no effect on dystrophin cluster density, or on the density of CB1- and VGLUT3-positive terminals (dystrophin: t_4=0.754, p=0.4927; CB1: t_4=1.089, p=0.3373; VGLUT3: t_4=0.1917, p=0.8573; unpaired t-test; Table 2).

Taken together, we conclude that targeted deletion of *Gabra1* causes moderate adaptations of GABAergic synapses in CA1 pyramidal cells. In the PCL, the absence of α1-$GABA_AR$ induces an increase in the density of synapses containing the α2 subunit and and gephyrin. These synapses likely originate from PV-basket cells, in view of the unchanged density of

VGLUT3-/CB1-positive terminals. Further, in both the PCL and RAD, the α2 subunit substitutes for the missing α1 subunit, as noted above. These postsynaptic densities contain a higher density of NL2, but not gephyrin, molecules. Since PV is distributed throughout GABAergic axons and not restricted to the terminal boutons, we did not use this marker to quantify the density of synapses made by PV-positive interneurons.

NL2-KO mice

To determine how the loss of NL2 affects the molecular organization and distribution of GABAergic synapses, we examined immunohistochemically the distribution of presynaptic and postsynaptic proteins in hippocampal formation of adult mice. In contrast with previous reports (Poulopoulos et al. 2009), the loss of NL2 had an effect on PSD protein clustering not only in the PCL but also in RAD. In addition, our analysis unraveled an unsuspected inter- and intra-animal variability in the severity of the effect, ranging from no detectable effect to severe loss for each of the postsynaptic proteins tested in NL2-KO. As the methods were the same as for analyzing α1-KO (or previously α2-KO) mice, this variability was apparently unique to NL2-KO mice. To illustrate this point, we tabulated the percentage change in the numerical density of α1 and α2 subunit, gephyrin, and dystrophin clusters in individual NL2-KO mice from four distinct litters compared to wildtype siblings analyzed at the same time and processed under identical conditions (Table 3). Although these four markers were not analyzed in all mice, it was remarkable to observe a strong divergence in the reduction of these postsynaptic markers within any given mutant mouse, irrespective of their sex. Overall, the trend was towards a severe reduction of α2 subunit clusters in the PCL in three mice, moderate in two mice and absent in two mice. In the RAD, 2 out of 5 mice had a moderate reduction and three were unchanged. For the α1 subunit, the reduction in the density of clusters was severe in only one mouse, moderate in six mice, and unchanged in two mice in the PCL. In the RAD, 5 out of 6 mice had a moderate reduction and one mouse was unchanged. Gephyrin clustering was the most severely affected, ranging from 8-85% of control in the PCL and 6-78% in the RAD. Remarkably, however, mice with a severe loss of

gephyrin clusters were not always the same as for the α2 subunit. Dystrophin clustering in the PCL was analyzed in five mice from three distinct litters. One had a severe reduction, one a moderate reduction and three were unchanged. These differential effects are illustrated in Figure 3 for gephyrin and the α1 subunit in the mice labeled KO1 and KO2 in Table 3, whereas the α2 subunit and dystrophin, co-stained along with VGAT, are illustrated for mouse KO1 in Figure 4. Despite this variability, statistical analysis pooling all mutants and controls revealed a significant reduction of the α2 subunit cluster density only in PCL.

These results were puzzling, as they might indicate technical issues with tissue preparation or staining. However, this was unlikely, because the technical procedure was exactly the same, and performed by the same person (PP) as for the analysis of α1-KO mice. In addition, the quality of sections and staining was very good in all mice selected for analysis, as illustrated (Fig. 3-4). To explore this issue further and determine whether the loss of a single NL2 allele would have an effect, we quantified the distribution of postsynaptic markers in the CA1 region of $NL2^{+/0}$ mice. The results showed that these heterozygotes were similar to their wildtype siblings (Table 4), with a similar degree of variability.

Next, we analyzed the effect of NL2 gene inactivation on the expression and distribution of markers of presynaptic terminals. VGAT was co-stained with postsynaptic markers (α2 subunit, dystrophin; Fig. 4), whereas CB1 and VGLUT3 were co-stained with dystrophin (Fig. 5). Quantitative analysis of the three GABAergic presynaptic markers analyzed revealed no effect of NL2 deletion (Table 5) on GABAergic synapse formation. Strikingly, comparison with Table 2 shows that the overall density of VGAT-positive terminals in NL2-KO mice and their wildtype littermates was only about 50% of that observed in the α1-KO mice – originally generated with a mixture of three strains (129/Sv/SvJ, C57BL/6J,FVB/N) (Kralic et al. 2002) – denoting strong strain differences in the density of GABAergic terminals in CA1.

Taken together, these results indicate that deletion of NL2 exerts highly variable effects on the postsynaptic clustering of $GABA_AR$ subunits, gephyrin and, to a lesser extent, dystrophin,

without affecting the differentiation of presynaptic terminals or the formation of synaptic junctions. We could not confirm the selective loss of perisomatic postsynaptic markers reported previously and found no evidence for a preferential association of NL2 with α1-$GABA_AR$. Rather, NL2 gene inactivation had the largest observable effect on postsynaptic clustering of gephyrin and the α2 subunit.

Discussion

The results demonstrate that targeted deletion of *Gabra1* causes an increase in the density of GABAergic markers in the PCL and RAD, in conjunction with an increase in presynaptic terminals from interneurons other than the CCK-basket cells. This finding confirms previous reports of increased α2 subunit expression in α1-KO mice (Kralic et al. 2006; Zeller et al. 2008; Schneider Gasser et al. 2007), but stands in striking contrast to the results from α2-KO mice, which revealed reduced frequency of mIPSCs and disruption of gephyrin postsynaptic clustering, without change in the density of GABAergic presynaptic terminals. Therefore, the constitutive absence of these two α subunit variants induces remarkably divergent effects on GABAergic synapse formation and molecular composition. In part, these differences might reflect differential properties of the α1 and α2 subunits with regard to their ability to regulate the formation of GABAergic synapses, as reported in heterologous expression systems (Brown et al. 2016).

The increased density of α2 subunit and gephyrin clusters observed in adult α1-KO mice likely represents a compensatory adaptation to the constitutive absence of a major $GABA_AR$ subtype. The increase is larger than that seen for VGAT terminals, which suggests that the α2 subunit replaces the α1 subunit in some synapses and that existing terminals might form additional release sites. We have shown previously that such compensation occurs in multiple interneuron types in the CA1 (Schneider Gasser et al. 2007). As we have no direct evidence of the cellular localization of the supernumerary α2 subunit and gephyrin clusters seen in the current study, it is conceivable that at least some of them are formed onto interneurons.

This compensation somewhat obscures the molecular reorganization occurring in various types of GABAergic synapses in the absence of α1-$GABA_ARs$, which we aimed to clarify in this study. Nevertheless, we can derive several conclusions from our results:

First, formation of postsynaptic clusters of dystrophin (as marker of the DGC) occurs independently of the expression or presence of the α1 subunit, confirming previous

speculations that $GABA_AR$ are dispensable for the selective localization of the DGC in GABAergic PSDs (Brünig et al. 2002).

Second, we interpret the increased slope of the intensity/size correlation of α2 subunit clusters in α1-KO mice as evidence that the α2 subunit replaces the α1 subunit in synapses where they normally are co-expressed. This increase in the number of α2 subunit proteins per synapse suggests that the size of GABAergic PSD is fixed and that PSDs can accommodate variable densities of α2-$GABA_AR$ and NL2 molecules, whereas the average density of gephyrin molecules appears invariable. If correct, this hypothesis implies that the packing density of α2-$GABA_ARs$ in the PSD can be higher than that of α1-$GABA_ARs$, possibly reflecting differences in mobility and/or binding to anchoring molecules.

Third, initial quantitative electron microscopy analyses had suggested a segregation of α1- and α2-$GABA_A$ receptors in perisomatic synapses from PV- and CCK-basket cells (Nyiri et al. 2001), respectively. Application of more sensitive methods, both in light and electron microscopy, could not confirm this observation (Panzanelli et al. 2011; Kasugai et al. 2010), and a recent report suggests that both subunits are present in the majority of GABAergic synapses, with a unimodal distribution across subcellular location (Kerti-Szigeti and Nusser 2016). This report raises the fundamental issue whether the two subunits are present within the same pentameric complex, or whether synapses contain distinct α1- and α2-$GABA_ARs$, each containing two molecules of the same variant. The former possibility would explain the increased intensity/size correlation of α2 subunit clusters discussed in the previous paragraph, but would imply that all GABAergic synapses have identical pharmacological and kinetics properties, which is highly unlikely. The latter possibility appears more plausible for this reason and because the possibility to insert variable amounts of two distinct receptor subtypes offers more room for functional plasticity.

Fourth, immunoelectron microscopy analysis demonstrated that terminals from CCK basket cells expressing VGLUT3 form specialized, invaginating synapses on the soma of pyramidal cells, highly enriched with cannabinoid signaling molecules, possibly activated upon glutamate release and binding to mGluRs (Omiya et al. 2015). Preservation of VGLUT3/CB1-

positive terminals, along with dystrophin clusters, strongly suggests that these synapses are not affected (or increased) in α1-KO mice (besides a change in the subunit composition of $GABA_AR$). Using immunofluorescence, we could not confirm a preferential localization of dystrophin apposed to VGLUT3-positive terminals, but the resolution of confocal microscopy might be insufficient to draw definitive conclusions. We have shown recently that genetic inactivation of dystroglycan has little effect on clustering of GABAergic PSD proteins, but prevents the formation (and maintenance) of synaptic terminals from CCK-basket cells and results in reduced GABAergic transmission in CA1 pyramidal cells(Früh et al. 2016). It is unknown whether the DGC contributes to the formation of invaginated synapses or to the postsynaptic anchoring of endocannabinoid synthesizing molecules.

Phenotypic variability of NL2-KO mice

The highly variable and divergent effects of NL2-gene inactivation observed here are unexpected and require careful consideration. The most immediate explanation is of technical nature and suggests that immunohistochemical detection of the proteins of interest was impaired for methodological reasons. However, this possibility is unlikely given that such problems did not arise with the analysis of α1-KO and NL2-heterozygote mice, processed in parallel and under exactly the same conditions. Further, if the mutation should affect immunohistochemical protein detection, the effect would be restricted to postsynaptic proteins, since we had no such variability in the staining of presynaptic markers. After having analyzed nine mutants in four distinct experiments, along with seven heterozygous mutants, we concluded that the variability was most likely to have a biological foundation.

Irrespective of this variability, we obtained no clear evidence for a preferential loss of GABAergic postsynaptic markers in the PCL compared to the RAD, unlike published results. One possible reason for this discrepancy is genetic drift between our colony of NL2-mutant mice and the original colony in the laboratory of Dr. Nils Brose at the Max-Planck Institute for Experimental Medicine in Göttingen (Germany). For this reason, we obtained from them a second lot of animals, which turned out to be identical to the first lot, making this hypothesis

improbable. An alternative explanation might be the increased sensitivity of our immunohistochemical procedure, which was designed to optimize the preservation of tissue following a mild fixation, as shown ultrastructurally (Notter et al. 2014).

Therefore, targeted inactivation of NL2 alters postsynaptic clustering of gephyrin, $GABA_AR$ and dystrophin. The inner- and inter-individual variability might be taken as evidence that the mechanisms underlying clustering of PSD proteins are not irreversibly impaired, but become dysfunctional and/or instable. It would be of interest to perform single-molecule tracking experiments in neuronal cultures of NL2-KO mice to determine whether kinetic parameters such as synaptic retention time and mean square displacement are impaired. A current model postulates interaction between NL2 and collybistin isoforms containing the SH3 domain for initiating the formation of a postsynaptic cluster (Soykan et al. 2014; Poulopoulos et al. 2009). Our results indicate that alternative mechanisms exist to compensate for the absence of NL2, notably a possible compensation by another neuroligin isoform (Varoqueaux et al. 2006; Hoon et al. 2011). Alterations in the splicing machinery of collybistin favoring retention of the SH3 domains might occur in NL2-KO mice.

Importantly, despite its indirect interaction with the DGC via S-SCAM and SynArfGEF binding to dystrophin (Sumita et al. 2007; Fukaya et al. 2011), NL2 does not appear to play a role in synapse formation, in striking contrast with our results that α-dystroglycan is required for formation and maintenance of synapses from CCK-basket cells (Früh et al. 2016). This finding further underlines the specificity of the dystroglycan-CCK-terminal trans-synaptic interaction and points towards distinct presynaptic binding partners of dystroglycan and NL2 in this context.

Taken together, the results confirm the pre-eminent role of NL2 as organizer of the GABAergic PSD; they provide no evidence for a preferential interaction with the DGC and/or α1-$GABA_AR$ (which we postulated to explain why NL2 and α1 subunit clustering is preserved in synapses containing the DGC of α2-KO mice). In contrast, α1-$GABA_AR$ contribute to regulate GABAergic synapse formation but are dispensable for clustering of postsynaptic proteins of the GABAergic PSD.

References

Baudouin S (2014) Heterogeneity and convergence: the synaptic pathophysiology of autism. Eur J Neurosci 39:1107-1113

Benke D, Honer M, Michel C, Mohler H (1996) GABAA receptor subtypes differentiated by their gamma-subunit variants: prevalence, pharmacology and subunit architercture. Neuropharmacol 35:1413-1422

Benke D, Mertens S, Trzeciak A, Gillessen D, Mohler H (1991) GABAA receptors display association of gamma2-subunit with alpha1- and beta2/3 subunits. J Biol Chem 266:4478-4483

Brown L, Nicholson M, Arama J, Mercer A, Thomson A, Jovanovic J (2016) γ-Aminobutyric Acid Type A ($GABA_A$) Receptor Subunits Play a Direct Structural Role in Synaptic Contact Formation via Their N-terminal Extracellular Domains. J Biol Chem 291:13926-13942

Brünig I, Suter A, Knuesel I, Luscher B, Fritschy JM (2002) GABAergic presynaptic terminals are required for postsynaptic clustering of dystrophin, but not of $GABA_A$ receptors and gephyrin. J Neurosci 22:4805-4813

Budreck EC, Scheiffele P (2007) Neuroligin-3 is a neuronal adhesion protein at GABAergic and glutamatergic synapses. Eur J Neurosci 26:1738-1748

Celio MR (1990) Calbindin D-28k and parvalbumin in the rat nervous system. Neuroscience 35:375-475

Dumoulin A, Rostaing P, Bedet C, Levi S, Isambert MF, Henry JP, Triller A, Gasnier B (1999) Presence of the vesicular inhibitory amino acid transporter in GABAergic and glycinergic synaptic terminal boutons. J Cell Sci 112:811-823

Fremeau RT, Burman J, Qureshi T, Tran CH, Proctor J, Johnson JA, Zhang H, Sulzer D, Copenhagen DR, Storm-Mathisen J, Reimer RJ, Chaudhry FA, Edwards RH (2002) The identification of vesicular glutamate transporter 3 suggests novel modes of signaling by glutamate. Proc Natl Acad Sci USA 99 (22):14488-14493

Fritschy JM, Mohler H (1995) $GABA_A$-receptor heterogeneity in the adult rat brain: differential regional and cellular distribution of seven major subunits. J Comp Neurol 359:154-194

Fritschy JM, Panzanelli P, Tyagarajan SK (2012) Molecular and functional heterogeneity of GABAergic synapses. Cell Mol Life Sci 69:2485-2499

Früh S, Romanos J, Panzanelli P, Bürgisser D, Tyagarajan S, Campbell K, Santello M, Fritschy J (2016) Neuronal Dystroglycan Is Necessary for Formation and Maintenance of Functional CCK-Positive Basket Cell Terminals on Pyramidal Cells. J Neurosci 36:10296-10313

Fukaya M, Kamata A, Hara Y, Tamaki H, Katsumata O, Ito N, Takeda S, Hata Y, Suzuki T, Watanabe M, Harvey RJ, Sakagami H (2011) SynArfGEF is a guanine nucleotide exchange factor for Arf6 and localizes preferentially at post-synaptic specializations of inhibitory synapses. J Neurochem 116:1122-1137

Gunther U, Benson J, Benke D, Fritschy JM, Reyes GH, Knoflach F, Crestani F, Aguzzi A, Arigoni M, Lang Y, Bluethmann H, Mohler H, Luscher B (1995) Benzodiazepine-insensitive mice generated by targeted disruption of the γ2-subunit gene of γ-aminobutyric acid type A receptors. Proc Natl Acad Sci USA 92:7749-7753

Hoon M, Soykan T, Falkenburger BH, Hammer M, Patrizi A, Schmidt KF, Sassoè-Pognetto M, Löwel S, Moser T, Taschenberger H, Brose N, Varoqueaux F (2011) Neuroligin-4 is localized to glycinergic postsynapses and regulates inhibition in the retina. Proc Natl Acad Sci USA 108:3053-3058

Kasugai Y, Swinny JD, Roberts JD, Dalezios Y, Fukazawa Y, Sieghart W, Shigemoto R, Somogyi P (2010) Quantitative localisation of synaptic and extrasynaptic $GABA_A$ receptor subunits on hippocampal pyramidal cells by freeze-fracture replica immunolabelling. Eur J Neurosci 32 (11):1868-1888

Kerti-Szigeti K, Nusser Z (2016) Similar $GABA_A$ receptor subunit composition in somatic and axon initial segment synapses of hippocampal pyramidal cells. Elife 5:e18426

Klausberger T, Marton L, O'Neill J, Huck J, Dalezios Y, Fuentealba P, Suen WY, Papp E, Kaneko T, Watanabe M, Csicsvari J, Somogyi P (2005) Complementary roles of cholecystokinin- and parvalbumin-expressing GABAergic neurons in hippocampal network oscillations. J Neurosci 25:9782-9793

Knuesel I, Mastrocola M, Zuellig RA, Bornhauser B, Schaub MC, Fritschy JM (1999) Altered synaptic clustering of $GABA_A$-receptors in mice lacking dystrophin (*mdx* mice). Eur J Neurosci 11:4457-4462

Knuesel I, Züllig RA, Bornhauser B, Schaub MC, Fritschy JM (2000) Differential expression of utrophin and dystrophin in CNS neurons: an in situ hybridization and immunohistochemical study. J Comp Neurol 422:594-611

Kralic JE, Korpi ER, O'Buckley TK, Homanics GE, Morrow A (2002) Molecular and pharmacological characterization of $GABA_A$ receptor α1 subunit knockout mice. J Pharmacol Exp Ther 302 (3):1037-1045

Kralic JE, Sidler C, Parpan F, Homanics G, Morrow AL, Fritschy JM (2006) Compensatory alteration of inhibitory synaptic circuits in thalamus and cerebellum of $GABA_A$ receptor α1 subunit knockout mice. J Comp Neurol 495:408-421

Lagier S, Panzanelli P, Russo RE, Nissant A, Bathellier B, Sassoè-Pognetto M, Fritschy JM, Lledo PM (2007) GABAergic inhibition at dendrodendritic synapses tunes γ oscillations in the olfactory bulb. Proc Natl Acad Sci USA 104:7259-7264

Lardi-Studler B, Smolinsky B, Petitjean CM, Koenig F, Sidler C, Meier JC, Fritschy JM, Schwarz G (2007) Vertebrate-specific sequences in the gephyrin E-domain regulate cytosolic aggregation and postsynaptic clustering. J Cell Biol 120:1371-1382

Morini R, Ghirardini E, Butti E, Verderio C, Martino G, Matteoli M (2015) Subventricular zone neural progenitors reverse TNF-alpha effects in cortical neurons. Stem cell research and Therapy 6:166

Notter T, Panzanelli P, Pfister S, Mircsof D, Fritschy J (2014) A protocol for concurrent high-quality immunohistochemical and biochemical analyses in adult mouse central nervous system. Eur J Neurosci 39:165-175

Nyiri G, Freund TF, Somogyi P (2001) Input-dependent synaptic targeting of α2-subunit-containing $GABA_A$ receptors in synapses of hippocampal pyramidal cells of the rat. Eur J Neurosci 13 (3):428-442

Omiya Y, Uchigashima M, Konno K, Yamasaki M, Miyazaki T, Yoshida T, Kusumi I, Watanabe M (2015) VGluT3-expressing CCK-positive basket cells construct invaginating synapses enriched with endocannabinoid signaling proteins in particular cortical and cortex-like amygdaloid regions of mouse brains. J Neurosci 35:4215-4228

Panzanelli P, Bardy C, Nissant A, Pallotto M, Sassoè-Pognetto M, Lledo PM, Fritschy JM (2009) Early synapse formation in developing interneurons of the adult olfactory bulb. J Neurosci 29:15039-15052

Panzanelli P, Gunn BG, Schlatter MC, Benke D, Tyagarajan SK, Scheiffele P, Belelli D, Lambert JJ, Rudolph U, Fritschy JM (2011) Distinct mechanisms regulate $GABA_A$ receptor and gephyrin clustering at perisomatic and axo-axonic synapses on CA1 pyramidal cells. J Physiol 589:4959-4980

Poulopoulos A, Aramuni G, Meyer G, Soykan T, Hoon M, Papadopoulos T, Zhang M, Paarmann I, Fuchs C, Harvey K, Jedlicka P, Schwarzacher SW, Betz H, Harvey RJ, Brose N, Zhang W, Varoqueaux F (2009) Neuroligin 2 drives postsynaptic assembly at perisomatic inhibitory synapses through gephyrin and collybistin. Neuron 63:628-642

Sassoè-Pognetto M, Fritschy JM (2000) Gephyrin, a major postsynaptic protein of GABAergic synapses. Eur J Neurosci 7:2205-2210

Schneider Gasser EM, Duveau V, Prenosil GA, Fritschy JM (2007) Reorganization of GABAergic circuits maintains $GABA_A$ receptor-mediated transmission onto CA1 interneurons in $\alpha 1-$subunit-null mice. Eur J Neurosci 25:3287-3304

Schneider Gasser EM, Straub CJ, Panzanelli P, Weinmann O, Sassoè-Pognetto M, Fritschy JM (2006) Immunofluorescence in brain sections: simultaneous detection of presynaptic and postsynaptic proteins in identified neurons. Nature Protocols 1:1887-1897

Soykan T, Schneeberger D, Tria G, Buechner C, Bader N, Svergun D, Tessmer I, Poulopoulos A, Papadopoulos T, Varoqueaux F, Schindelin H, Brose N (2014) A conformational switch in collybistin determines the differentiation of inhibitory postsynapses. EMBO J 33:2113-2133

Sumita K, Sato Y, Iida J, Kawata A, Hamano M, Hirabayashi S, Ohno K, Peles E, Hata Y (2007) Synaptic scaffolding molecule (S-SCAM) membrane-associated guanylate kinase with inverted organization (MAGI)-2 is associated with cell adhesion molecules at inhibitory synapses in rat hippocampal neurons. J Neurochem 100:154-166

Tyagarajan SK, Fritschy JM (2014) Gephyrin, a master regulator of neuronal function? Nature Rev Neurosci 15:141-156

Varoqueaux F, Aramuni G, Rawson RL, Mohrmann R, Missler M, Gottmann K, Zhang W, Suedhof TC, Brose N (2006) Neuroligins determine synapse maturation and function. Neuron 51:741-754

Waite A, Brown SC, Blake DJ (2012) The dystrophin-glycoprotein complex in brain development and disease. Trends Neurosci 35:487-496

Waite A, Tinsley CL, Locke M, Blake DJ (2009) The neurobiology of the dystrophin-associated glycoprotein complex. Ann Med 41:344-359

Zeller A, Crestani F, Camenisch I, Iwasato T, Itohara S, Fritschy J, Rudolph U (2008) Cortical glutamatergic neurons mediate the motor sedative action of diazepam. Mol Pharmacol 73:282-291

Tables

Table 1: List of primary antibodies

Target protein	Species	Dilution	Source; Catalog
$GABA_AR$ α1 subunit	Rabbit, Guinea pig	1:20000	Self-made
$GABA_AR$ α2 subunit	Guinea pig	1:1000	Self-made
Gephyrin	Mouse	1:700	Synaptic Systems; mAb7a; 147011
VGAT	Rabbit	1:3000	Synaptic Systems; 131003
VGLUT3	Guinea pig	1:2000	Millipore, AB5421
CB1	Rabbit	1:3000	Synaptic System; 258 003
Dystrophin Rod Domain	Mouse	1:100	Novocastra NCL-Dys 1
Neuroligin-2	Rabbit	1:10000	Received from Dr. P. Scheiffele
Parvalbumin	Mouse	1:5000	Swant 235

Table 2

Quantification of presynaptic and postsynaptic clustering in CA1 of α1-KO mice

α1-KO	PCL						RAD					
	Cluster density (1000 μm²)		Cluster size (μm²)		Slope (95% CI) of size-intensity correlation		Cluster density (1000 μm²)		Cluster size (μm²)		Slope (95% CI) of size-intensity correlation	
	WT	**KO**	**WT**	**KO**	**WT**	**KO**	**WT**	**KO**	**WT**	**KO**	**WT**	**KO**
α2	**70±2**	**93±2****	0.3± 0.004	0.4± 0.005	**120-121**	**135-137**	**65±2**	**84±4****	0.3± 0.003	0.3± 0.003	**115-116**	**133-134**
NL2	109±5	102±6	0.3± 0.003	0.3± 0.004	**121-123**	**137-139**	92±5	105±7	0.3± 0.002	0.3± 0.003	**118-119**	**135-136**
Gephyrin	**64±2**	**90±3****	0.2± 0.003	0.2± 0.004	98-100	94-96	**76±2**	**114±1****	0.2± 0.002	0.2± 0.002	119-120	115-116
VGAT	**254±12**	**299±3***	0.3± 0.005	0.3± 0.003			263±17	290±4	0.3± 0.003	0.3± 0.003		
Dystr	118±12	109±4	0.3± 0.005	0.4± 0.005	142-143	148-149						
VGLUT3	50±8	49±5	0.9± 0.01	1± 0.01								
CB1	51±8	62±5	n.d.	n.d.								

The values were determined in images from double and triple immunofluorescence staining with various combinations of markers. They are given as mean ± SEM for the stratum pyramidale (PCL) and stratum radiatum (RAD) of CA1 in wildtype (WT) and α1-KO mice. Values indicated in bold are significantly different between genotypes (*P<0.05; **P<0.01; ****P<0.0001; N=6 mice/genotype). n.d., not determined

Table 3

Variability in the density of clusters formed by postsynaptic markers in the CA1 area of NL2-KO mice

	PCL				RAD		
	geph	**α1**	**α2**	**dystr**	**geph**	**α1**	**α2**
KO1	14	31	43	38	26	88	47
KO2	85	55	98	108	78	48	109
KO3	8	41	108	136	8	33	43
KO4	10	17	11		6	53	82
KO5	41	116	81		14	63	79
KO6	61	36			55	50	
KO7	80	145			76		
KO8		73	79	92			
KO9		65	57	68			

Results are given for animals investigated in separate experiments (each color indicate a given experiment), obtained for the α1 and α2 subunit, gephyrin, and dystrophin. The numbers are the ratio (%) of cluster density in each NL2-KO mice relative to the mean density of wildtype littermates processed in the same experiment.

Table 4

Quantification of postynaptic cluster density in CA1 of $NL2^{+/0}$ mice

$NL2^{+/0}$	PCL		RAD	
	WT	**Het**	**WT**	**Het**
Geph N=7	55±14	73±24	58±18	62±21
α2 N=5	124±13	133±11	86±12	80±13
Dystr N=3	92±18	101±4		
α1 N=7	95±23	88±21	173±50	180±48

The numerical density of clusters per 1000 μm^2 is given as mean ± SEM in the stratum pyramidale (PCL) and stratum radiatum (RAD). No significant difference was observed between genotypes for any of the four markers (unpaired t-test).

Table 5

Quantification of presynaptic terminal density in CA1 of NL2-KO mice

NL2-KO	PCL			RAD		
	WT	**KO**	**Het**	**WT**	**KO**	**Het**
VGAT	121±13 N=6	144±24 N=5	100±6 N=3	172±14 N=6	150±31 N=5	109±23 N=3
VGLUT3	49±8 N=5	61±7 N=4	54±5 N=5			
CB1	64±4 N=5	76±8 N=4	80±5 N=5			

The numerical density of clusters per 1000 μm^2 is given as mean ± SEM in the stratum pyramidale (PCL) and stratum radiatum (RAD). No significant difference was observed between genotypes for any of the markers (ANOVA).

Figure legends

Figure 1

Differential alterations in postsynaptic marker distribution in CA1 neurons of α1-KO mice, as analyzed in perisomatic synapses of CA1 pyramidal cell layer. A-A''') Images from triple immunofluorescence for NL2 (green), α2 subunit (red), and gephyrin (blue) in wildtype mice, demonstrating the co-localization of these three proteins, as shown in a merged and in color-separated images. B-B'") Selective preservation of NL2 (green) which contrasts with the increase of α2 subunit (red), and gephyrin (blue) clustering. C-D') Quantification of α2 subunit and gephyrin cluster size, displayed by cumulative distribution analysis in stratum radiatum (RAD; C, D) and pyramidal cell layer (PCL; C', D'). An increase of α2 subunit cluster size was evident in both regions of mutant mice. E-F') Scatter plots of $GABA_AR$ α2 subunit cluster intensity versus size in RAD (E-E') and PCL (F-F'); the line indicates the slope of the correlation, which is increased in mutants for both regions (see Table 2).

Figure 2

Increased dystrophin clustering in perisomatic synapses of CA1 pyramidal cells in α1-KO mice. A-B'") Triple immunofluorescence for dystrophin (green), CB1 (red), and VGLUT3 (blue), illustrating the unaltered density of dystrophin clusters at presumptive perisomatic postsynaptic sites in α1-KO mice as well as of CB1- and VGLUT3-positive terminals arising from CCK basket cells, as shown in a merged and in color-separated images.

Figure 3

Phenotypic variability of gephyrin (green) and α1 subunit (red) clustering in the CA1 area of NL2-KO mice, as illustrated by double immunofluorescence staining in one wildtype mouse (A-A") and two NL2-KO littermates (B-C''). The mouse NL2KO1 exhibits severe loss of gephyrin clustering and moderate loss of α1 subunit clustering in the pyramidal cell layer while the mouse NL2KO2 shows no change in gephyrin clustering and a loss of α1 subunit clustering comparable to NL2KO1.

Figure 4

Images from triple immunofluorescence staining illustrating an example of moderately decreased α2 subunit clustering (red) along with preserved dystrophin clustering (green) and distribution of VGAT-positive terminals (blue) in the CA1 pyramidal cells layer of a NL2-KO mouse. (A-A'", wildtype; B-B'", NL2-KO).

Figure 5

Images from triple immunofluorescence staining depicting the unaltered density of clusters immunopositive for dystrophin (green), CB1 (red) and VGLUT3 (blue) in the CA1 area of a NL-2-KO mouse compared to a wildtype littermate. (A-A'", wildtype; B-B'", NL2-KO).

FIG 1

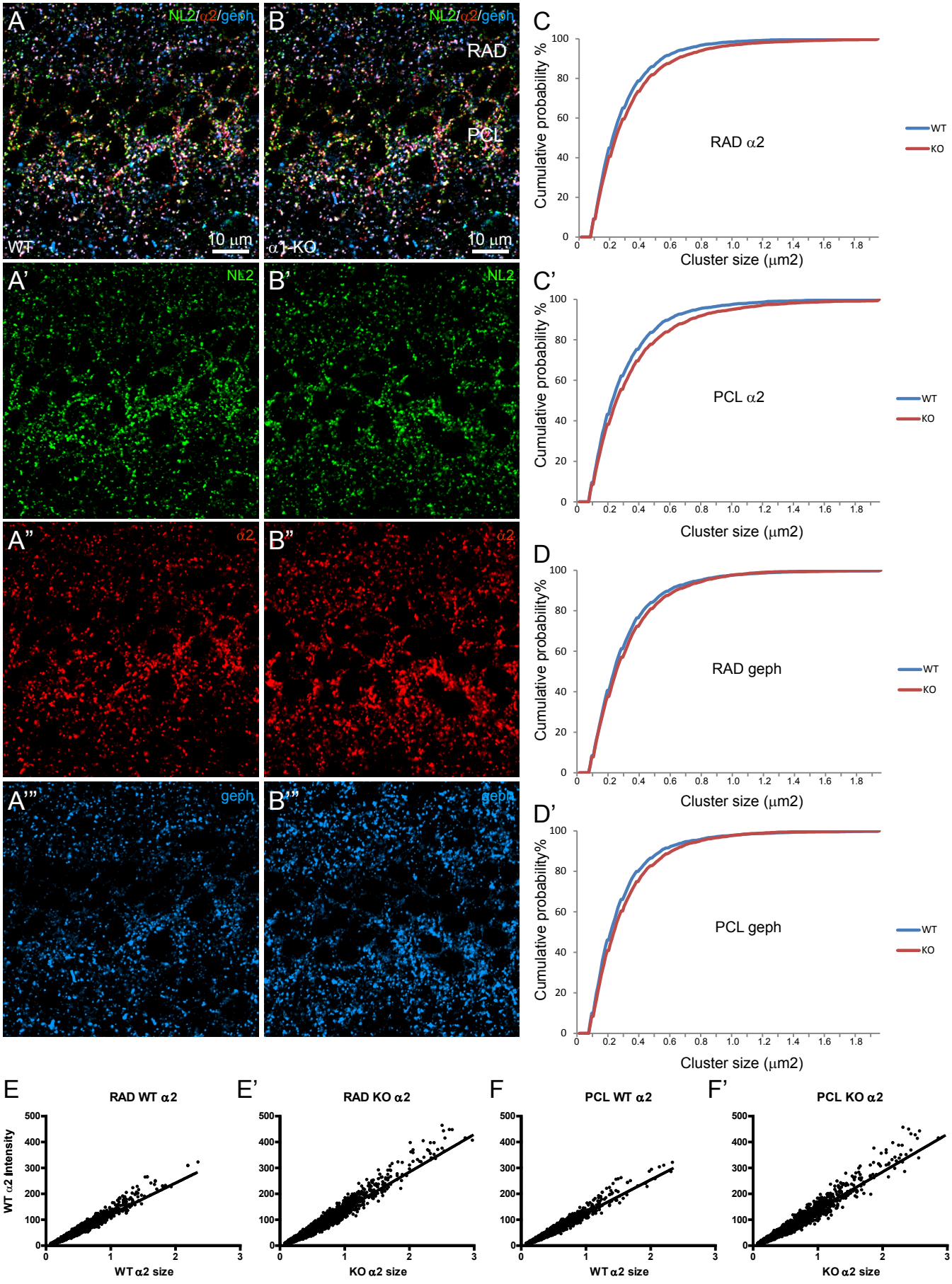
A
NL2/α2/geph
WT
10 μm
B
NL2/α2/geph
RAD
PCL
α1-KO
10 μm
A'
NL2
B'
NL2
A''
α2
B''
α2
A'''
geph
B'''
geph
C
Cumulative probability %
RAD α2
Cluster size (μm2)
WT
KO
C'
PCL α2
D
RAD geph
D'
PCL geph
E
RAD WT α2
WT α2 intensity
WT α2 size
E'
RAD KO α2
KO α2 size
F
PCL WT α2
F'
PCL KO α2

FIG 2

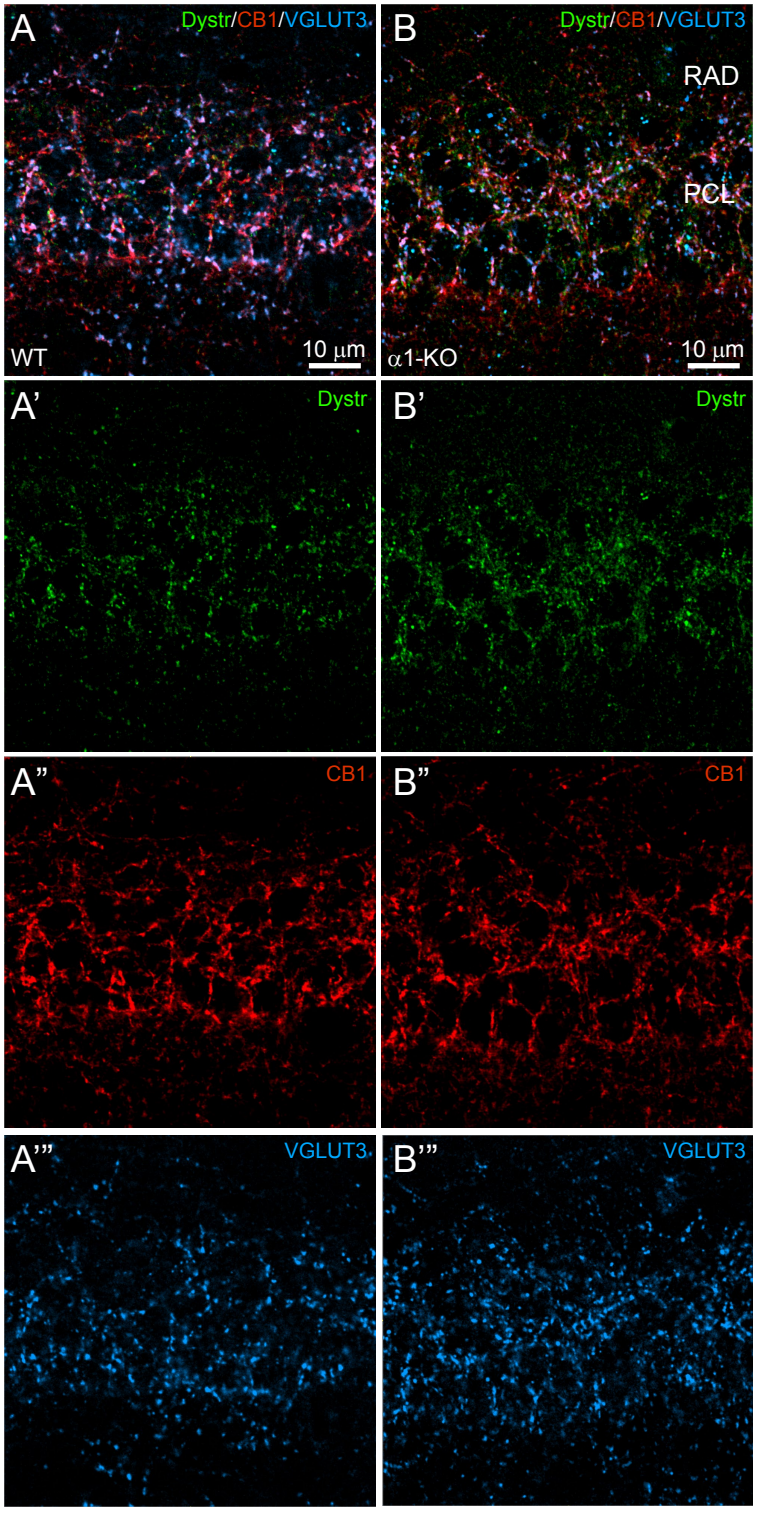
A
Dystr/CB1/VGLUT3
WT
10 μm
B
Dystr/CB1/VGLUT3
RAD
PCL
α1-KO
10 μm
A'
Dystr
B'
Dystr
A"
CB1
B"
CB1
A'"
VGLUT3
B'"
VGLUT3

FIG 3

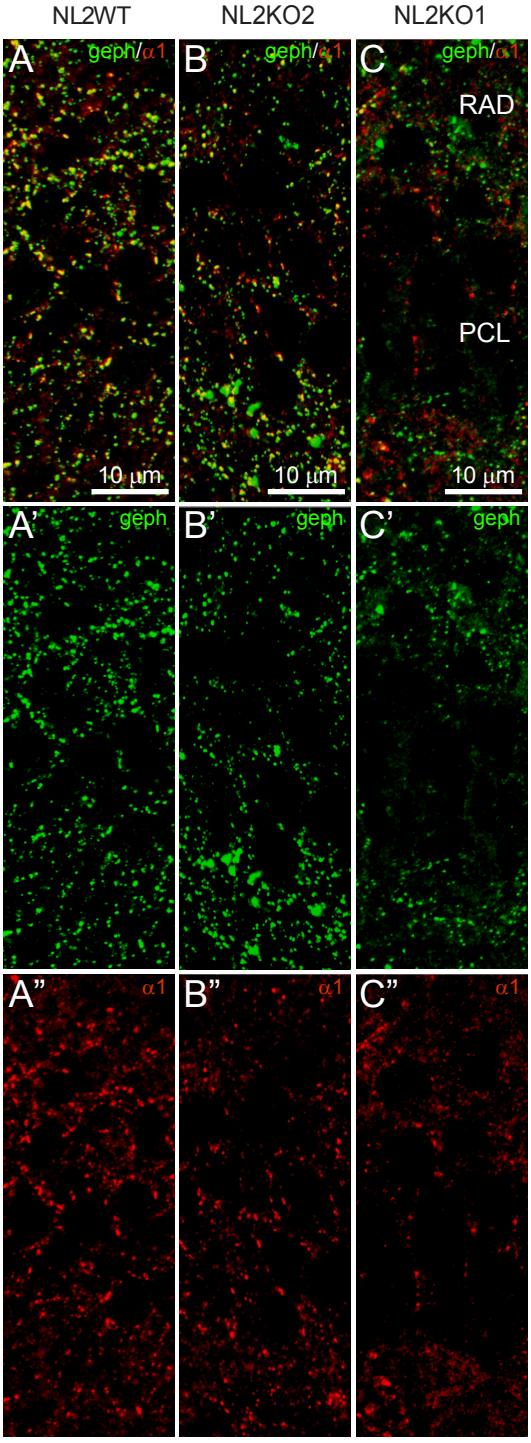
NL2WT
NL2KO2
NL2KO1
A
geph/α1
B
geph/α1
C
geph/α1
RAD
PCL
10 μm
10 μm
10 μm
A'
geph
B'
geph
C'
geph
A"
α1
B"
α1
C"
α1

FIG 4

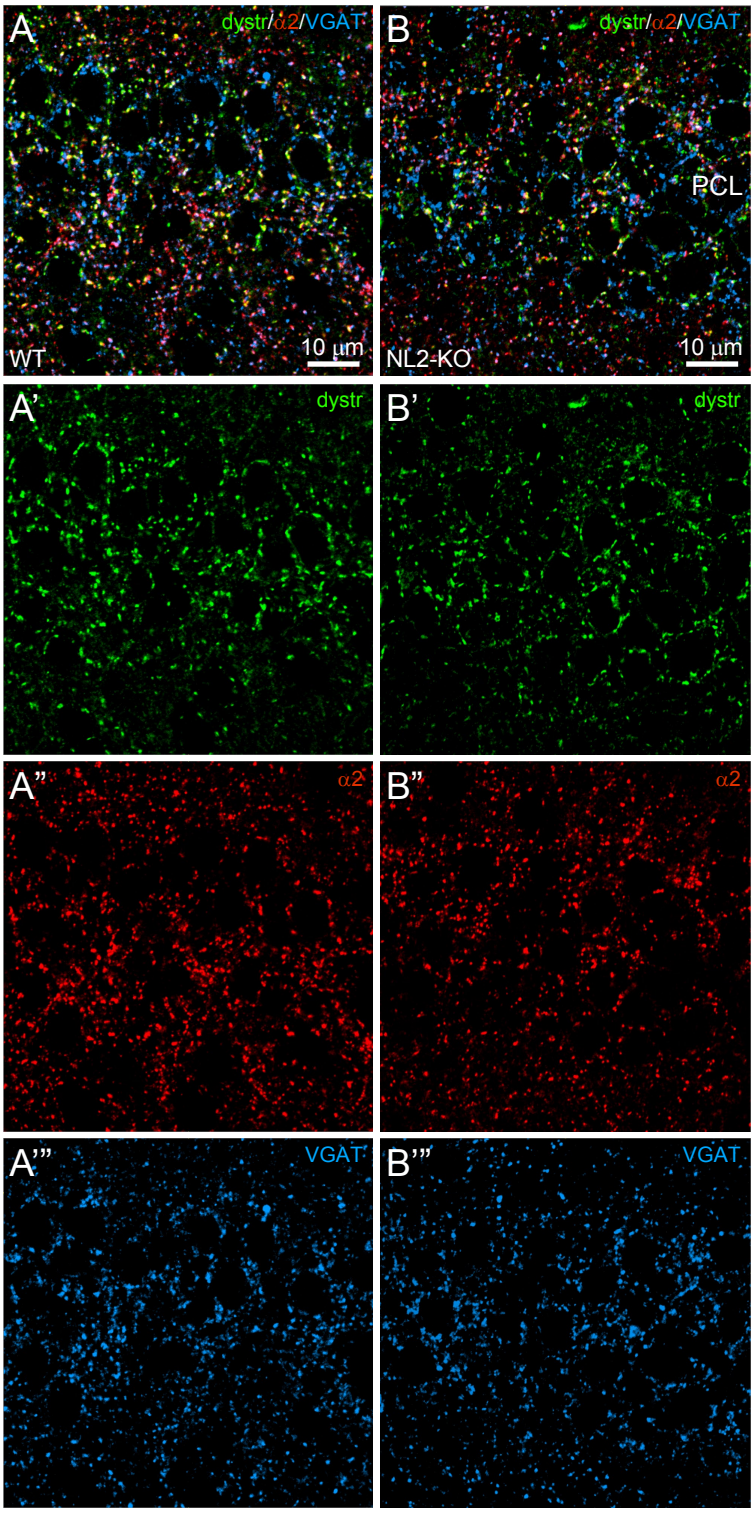
A
dystr/α2/VGAT
WT
10 µm
B
dystr/α2/VGAT
PCL
NL2-KO
10 µm
A'
dystr
B'
dystr
A''
α2
B''
α2
A'''
VGAT
B'''
VGAT

FIG 5

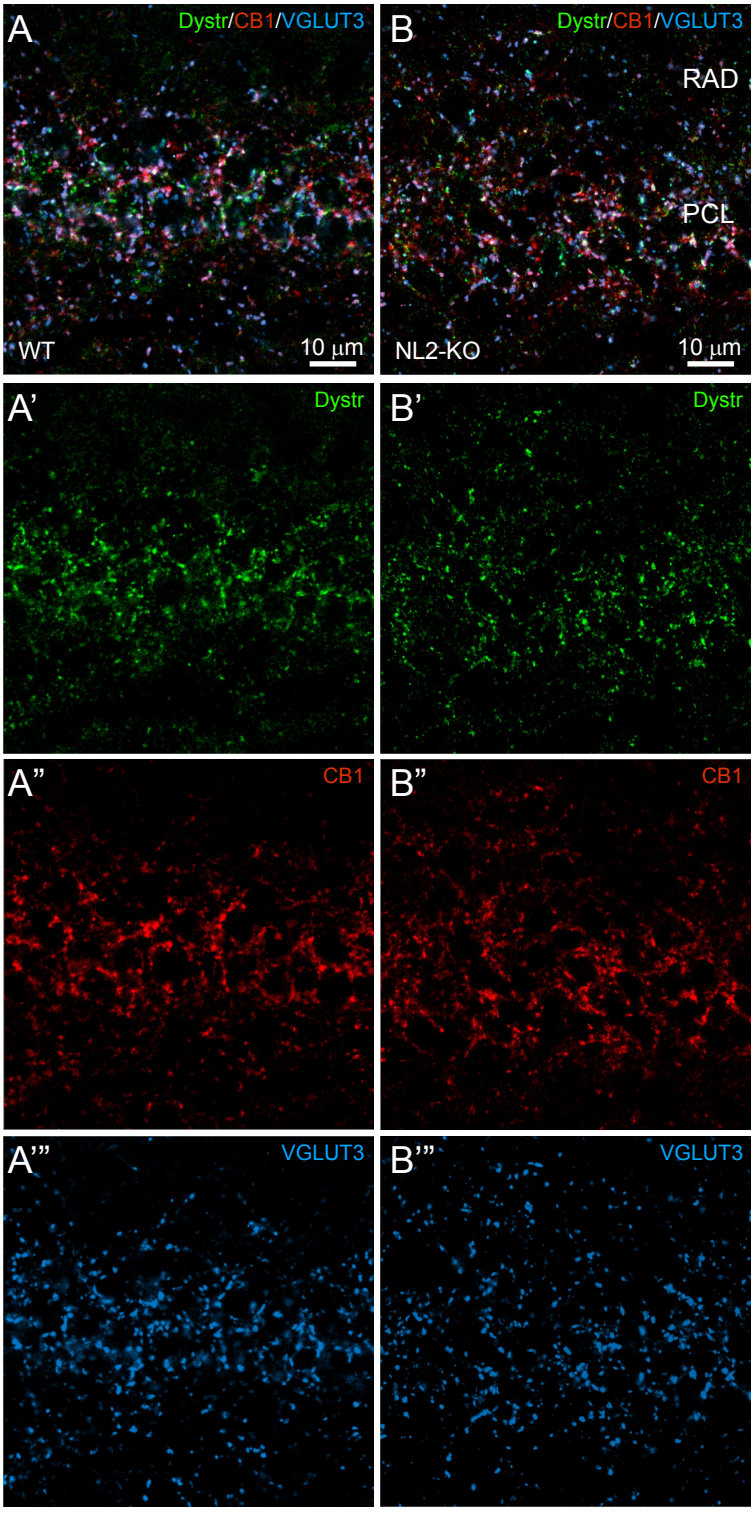
A
Dystr/CB1/VGLUT3
WT
10 μm
B
Dystr/CB1/VGLUT3
RAD
PCL
NL2-KO
10 μm
A'
Dystr
B'
Dystr
A"
CB1
B"
CB1
A'"
VGLUT3
B'"
VGLUT3